JOURNAL OF THEORETICAL
AND APPLIED MECHANICS
50, 1, pp. 251-268, Warsaw 2012
50th anniversary of JTAM

MODELING AND NUMERICAL SIMULATION OF UNMANNED AIRCRAFT VEHICLE RESTRICTED BY NON-HOLONOMIC CONSTRAINTS

Edyta Ładyżyńska-Kozdraś

Warsaw University of Technology, Faculty of Mechatronics, Warsaw, Poland

e-mail: e.ladyzynska@mech.pw.edu.pl

The paper presents the modeling of flight dynamics of an unmanned aircraft vehicle (UAV) using the Boltzmann-Hamel equations for mechanical systems with non-holonomic constraints. Control laws have been treated as non-holonomic constraints superimposed on dynamic equations of motion of UAV. The mathematical model containing coupling dynamics of the aircraft with superimposed guidance have been obtained by introducing kinematic relationships as the preset parameters of the motion resulting from the process of guidance. The correctness of the developed mathematical model was confirmed by the carried out numerical simulation.

Key words: automatically steered aircraft vehicle, non-holonomic constraints, Boltzmann-Hamel equations

1. Introduction

In recent years, unmanned aircraft vehicles (UAV) have been the fastest growing means of recognizing and supporting the armed forces. On the modern battlefield, light small-sized UAVs perform the mission of ground target detection, tracking and illumination. Their modified versions, combat UAVs, are supposed not only to autonomously detect the target, but also destroy it with on-deck homing missiles (Fig. 1). UAVs usefulness has been confirmed unequivocally both by operations carried out by the Americans in Iraq and Afghanistan, as well as Israeli military operations in Lebanon and Gaza. No wonder that acquiring a UAV for the Polish army has become one of the priorities of its technical modernization in the years 2009-2018. For the same reasons, the problems associated with the study of dynamics and control of the UAV is the focus of many scientific and research centres in Poland and the world. There are also many methods of modelling these issues from the equations of classical mechanics using the principle of changing angular momentum (Dogan and Venkataramanan, 2005; Ducard, 2009; Etkin and Reid, 1996; Maryniak, 2005; Rachman and Razali, 2011; Sadraey and Colgren, 2005), to the methods of analytical mechanics for nonholonomic systems. Analytical mechanics provides several methods of generating equations of motion of flying objects. Boltzmann-Hamel equations, as well as Maggi's, Gibbs-Appel, Keyn equations, and the projective method developed by Professor W. Blajer, used in the study, are among them (Blajer, 1998; Blajer *et al.*, 2001; Chelaru *et al.*, 2009; Graffstein *et al.*, 1997; Gutowski, 1971; Koruba and Ładyżyńska-Kozdraś, 2010; Ładyżyńska-Kozdraś, 2008, 2009, 2011; Maryniak, 2005; Sadraey and Colgren, 2005; Ye *et al.*, 2006).

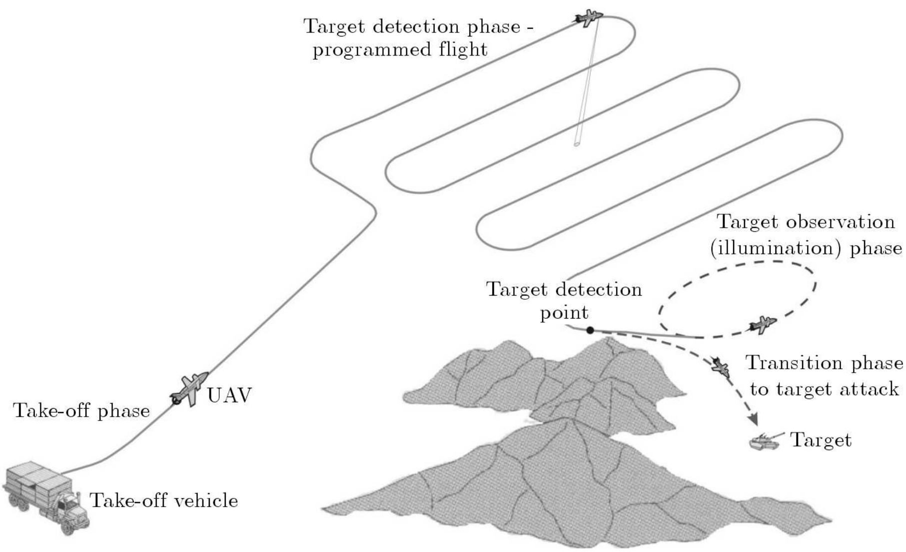

Fig. 1. General view of combat UAV mission performance (Koruba and Ładyżyńska-Kozdraś, 2010)

The dynamical modeling of UAV forms the heart of its simulation (Sadraey and Colgren, 2005). The numerical simulation of the aircraft dynamics is the most important tool in the development and verification of the flight control laws and equations of motion for a UAV. The ability to test autopilot systems in a virtual (software) environment using a software flight dynamics model for UAVs is significant for development, as shown for example in the work by Blajer *et al.* (2001), Chelaru *et al.* (2009), Dogan and Venkataramanan (2005), Jordan *et al.* (2006), Ładyżyńska-Kozdraś (2011), Ou *et al.* (2008), Shim *et* *al.* (2003). In many cases, testing newly developed autopilot systems in a virtual environment is the only way to guarantee absolute safety. Additionally, the model would allow better repeatability in testing, with controlled flying environments.

This study is a continuation and generalization of the article published in the Journal of Theoretical and Applied Mechanics (Koruba and Ładyżyńska-Kozdraś, 2010), where was proposed an algorithm of guiding combat UAV, which on having autonomously detected targets, attack them (e.g. radar stations, combat vehicles or tanks) or illuminate them with a laser (Fig. 1). The simplified equations of UAV motion developed there were now generalized for the object with nonholonomic constraints. In the article, a novel method was proposed based on treating the nonholonomic constraints as laws of controlling and conjugating them with nonlinear equations of motion of an object and with kinematic guidance relations (Ładyżyńska-Kozdraś, 2008, 2009, 2011).

Control, that is override aimed at ensuring that the moving object behaves in a desired manner, was brought to testing of differences, that is deviations between the required and actual value of the realized coordinate. The value of this difference, after appropriate strengthening and transforming, resets the deviation. Developed in this way control laws were treated as non-holonomic constraints superimposed on the motion of a UAV. Linkage of these equations with the dynamic equations of motion of the object made it possible, thanks to the use of Boltzmann-Hamel equations for mechanical systems with non-holonomic constraints, to control the flight of a UAV in an effective manner.

2. Physical model of UAV and adopted reference systems

The article presents the process of modeling and numerical simulation of the flight of unmanned aircraft vehicle during the mission. Appropriate formulation of the physical model is an important element here, which will constitute the basis for building a mathematical model of motion of the tested object.

The following assumptions of the physical model have been adopted:

- UAV is treated as a non-deformable object, with six degrees of freedom resulting from the movement of rudders;
- Motion of a UAV is examined in calm weather;
- UAV weight varies during the flight;
- UAV motion control may be carried out in four channels: in the pitch channel θ – by means of elevator deflections δ_H, in the yaw channel ψ

– by means of rudder deflections δ_V, in the roll channel ϕ – by means of aileron deflection δ_L, and in the speed channel V_0 – by changing the engine thrust δ_T;

- Control units are moving, but they are non-deformable;
- Deflection of surfaces of rudders affects the forces and moments of aerodynamic forces;
- Constraints superimposed on a UAV resulting from the adopted control laws have been treated as non-holonomic constraints;
- Forces and moments of aerodynamic forces, from the propulsion system and gravitation, act on the UAV;
- The impact of the curvature of the Earth was ignored;
- The environment has an impact on the dynamic properties of the drive through changes in air temperature t_H, air density ρ_H, air pressure p_H, kinematic viscosity ν_H, sound speed a_H depending on the altitude.

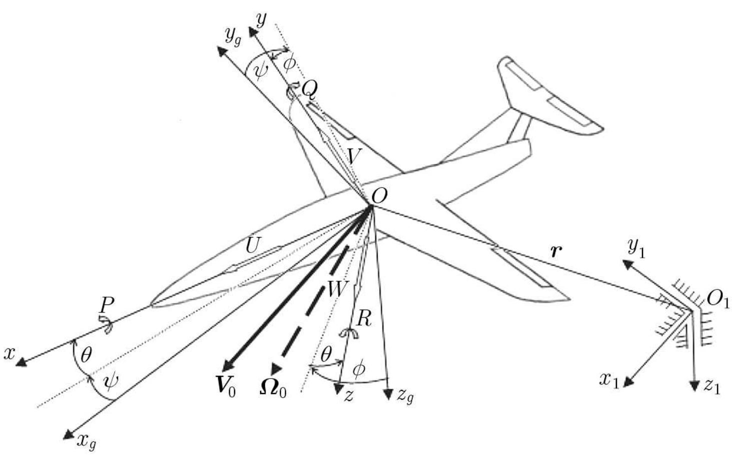

Fig. 2. Adopted reference systems, linear and angular speed of a UAV

The motion of a unmanned aircraft vehicle is examined in the reference system $Oxyz$, rigidly connected with the moving object, with the beginning in the center of mass of the UAV after burnup of fuel (Fig. 2). The other reference system used in the paper includes: system $O_1x_1y_1z_1$, rigidly connected with the Earth, as well as systems connected with the object, namely: gravitational $Ox_gy_gz_g$ parallel to $O_1x_1y_1z_1$ system and velocity $Ox_ay_az_a$ connected with the air flow direction (Fig. 3).

3. Kinematic correlations and guidance correlations

The motion of a unmanned aircraft vehicle during a mission is described with the use of coordinates and time in the space of events where the location of the object is uniquely determined with the use of linear and angular coordinates in the configuration space.

Pursued flight parameters of the UAV are read automatically by the guidance system and depend only on the actual behavior of the guided object on the track, and thus on the changes of its linear and angular position.

The vector of the actual linear velocity of the UAV (Fig. 2) in the $Oxyz$ system is

$$\boldsymbol{V}_0 = U\boldsymbol{i} + V\boldsymbol{j} + W\boldsymbol{k} \tag{3.1}$$

where: U, V, W are respectively: longitudinal, lateral and vertical velocity; $\boldsymbol{i}, \boldsymbol{j}, \boldsymbol{k}$ – unit vectors of the system associated with the $Oxyz$ object.

The angular velocity vector

$$\boldsymbol{\Omega} = P\boldsymbol{i} + Q\boldsymbol{j} + R\boldsymbol{k} \tag{3.2}$$

where: P, Q, R are the angular velocity of banking, tilt and deflection (Fig. 2).

Kinematic correlations between the components of angular velocities and derivatives of the angles have the following form (Blajer, 1998; Etkin and Reid, 1996; Ładyżyńska-Kozdraś, 2009, 2011)

$$\begin{bmatrix} \dot{\phi} \\ \dot{\theta} \\ \dot{\psi} \end{bmatrix} = \begin{bmatrix} 1 & \sin\phi\tan\theta & \cos\phi\tan\theta \\ 0 & \cos\phi & -\sin\phi \\ 0 & \sin\phi\sec\theta & \cos\phi\sec\theta \end{bmatrix} \begin{bmatrix} P \\ Q \\ R \end{bmatrix} \tag{3.3}$$

Kinematic correlations between the components of the linear velocity $\dot{x}_1, \dot{y}_1, \dot{z}_1$ measured in the system $O_1x_1y_1z_1$ rigidly connected with the Earth and the components of U, V, W velocity in the reference system $Oxyz$ associated with the moving objects are as follows (Blajer, 1998; Etkin and Reid, 1996; Ładyżyńska-Kozdraś, 2009, 2011)

$$\begin{bmatrix} \dot{x}_1 \\ \dot{y}_1 \\ \dot{z}_1 \end{bmatrix} = \begin{bmatrix} \cos\psi\cos\theta & \begin{matrix}\cos\psi\sin\theta\sin\phi+ \\ -\cos\phi\cos\psi\end{matrix} & \begin{matrix}\cos\psi\sin\theta\cos\phi+ \\ +\sin\phi\cos\psi\end{matrix} \\ \sin\psi\cos\theta & \begin{matrix}\sin\psi\sin\theta\sin\phi+ \\ -\sin\phi\cos\psi\end{matrix} & \begin{matrix}\sin\psi\sin\theta\cos\phi+ \\ -\sin\phi\cos\psi\end{matrix} \\ -\sin\theta & \sin\phi\cos\theta & \cos\phi\cos\theta \end{bmatrix} \begin{bmatrix} U \\ V \\ W \end{bmatrix} \tag{3.4}$$

In calm weather the angle of approach α and glide β are expressed by the following formulas (Blajer, 1998; Etkin and Reid, 1996; Ładyżyńska-Kozdraś, 2009, 2011):

— the angle of approach

$$\alpha = \arctan \frac{W}{U} \tag{3.5}$$

— the angle of glide

$$\beta = \arcsin \frac{V}{V_0} \tag{3.6}$$

Preset flight parameters of the unmanned aircraft result from the adopted guidance method. Assuming that during the observation of the area the aircraft flies along the pre-programmed route, constraints are superimposed on the location and angular and linear velocity of the object, thus creating the generator of its programmed motion (Blajer, 1998; Blajer *et al.*, 2001; Ładyżyńska-Kozdraś, 2011)

$$\begin{aligned} \widehat{K_0K_e} &= s(x_{1p}, y_{1p}, z_{1p}, \phi_p, \theta_p, \psi_p) \\ V_z(t) &= \dot{s}(\dot{x}_{1p}, \dot{y}_{1p}, \dot{z}_{1p}, \dot{\phi}_p, \dot{\theta}_p, \dot{\psi}_p, \phi_p, \theta_p, \psi_p) \end{aligned} \tag{3.7}$$

where: x_{1p}, y_{1p}, z_{1p}, ϕ_p, θ_p, ψ_p are the preset parameters of motion of the controlled object.

When the UAV detects the target, it is possible to trace or attack it. In this case, the preset parameters of the controlled object were selected in the paper with the use of one of self-guidance methods, that is the method of "along the curve of hunt" (Koruba and Ładyżyńska-Kozdraś, 2010; Ładyżyńska-Kozdraś, 2011). It assumes that the preset angular coordinates of the guided object are consistent with the parameters of the target

$$\phi_p = \phi_t \qquad \theta_p = \theta_t \qquad \psi_p = \psi_t \tag{3.8}$$

The vector of the preset location of UAV in $O_1x_1y_1z_1$ system (Fig. 2) is

$$\boldsymbol{r}_p = x_{1p}\boldsymbol{i}_1 + y_{1p}\boldsymbol{j}_1 + z_{1p}\boldsymbol{k}_1 \tag{3.9}$$

where

$$x_{1p} = r_{ot} \cos\psi_t \cos\theta_t \qquad y_{1p} = -r_{ot} \sin\psi_t \cos\theta_t \qquad z_{1p} = -r_{ot} \sin\theta_t$$

and r_{ot} is the distance of the actual location of the object to the target, ϕ_t, θ_t, ψ_t – angles of banking, tilt and deflection of the maneuvering target.

The components of the vector of the preset linear velocity of UAV in the own system are

$$\begin{bmatrix} U_p \\ V_p \\ W_p \end{bmatrix} = \begin{bmatrix} \cos\psi_t\cos\theta_t & \sin\psi_t\cos\theta_t & -\sin\theta_t \\ \begin{gathered}\sin\phi_t\cos\psi_t\sin\theta_t+ \\ -\sin\psi_t\cos\phi_t\end{gathered} & \begin{gathered}\sin\phi_t\sin\psi_t\sin\theta_t+ \\ +\cos\psi_t\cos\phi_t\end{gathered} & \sin\phi_t\cos\theta_t \\ \begin{gathered}\cos\phi_t\cos\psi_t\sin\theta_t+ \\ +\sin\psi_t\sin\phi_t\end{gathered} & \begin{gathered}\cos\phi_t\sin\psi_t\sin\theta_t+ \\ -\cos\psi_t\sin\phi_t\end{gathered} & \cos\phi_t\cos\theta_t \end{bmatrix} \begin{bmatrix} \dot{x}_{1p} \\ \dot{y}_{1p} \\ \dot{z}_{1p} \end{bmatrix} \tag{3.10}$$

The components of the vector of the preset angular velocity of UAV in the own system are

$$\begin{bmatrix} P_p \\ Q_p \\ R_p \end{bmatrix} = \begin{bmatrix} 1 & 0 & -\sin\theta_t \\ 0 & \cos\phi_t & \sin\phi_t\cos\theta_t \\ 0 & -\sin\phi_t & \cos\phi_t\cos\theta_t \end{bmatrix} \begin{bmatrix} \dot{\phi}_t \\ \dot{\theta}_t \\ \dot{\psi}_t \end{bmatrix} \tag{3.11}$$

During the flight of the unmanned aircraft, the preset parameters resulting from the adopted guidance method are compared with the parameters of the flight of the aircraft which are read on the ongoing basis. The differences which occur between these parameters are then removed by the automatic control system. In this way, the control mechanism affects motion of the object by means of relevant control units, depending on changes in one or, most often, many parameters of its motion.

4. Control laws

The motion of the unmanned aircraft along the preset trajectory results from the superimposed kinematic constraints. These constraints are, however, violated due to various external interferences, construction deficiencies, etc. It is therefore necessary to equip the object with a set of devices that will determine the degree of violation of these constraints and will generate appropriate control signals so that the aircraft will fly along the required track. All these tasks are pursued by the control system.

In this way, through the appropriate control units, the mechanism of automatic guidance of the object affects its movement, depending on one or, most often, many parameters such as acceleration, speed, linear and angular position, track angle. This affects the dynamics of the controlled object, causing a change of control forces which enforce the flight consistent with the adopted control system and guidance algorithm. The automatic control system, basing on the values of deviations which compare information about the state of the controlled object and the vector of the preset state, generates control signals. Kinematic and geometric deviations relationships in the servomechanisms become strengthened and then they are transferred to the actuators, such as hydraulic, electrohydraulic or electromechanical cylinders. The delay of the control system has been described by means of an inertial unit of the first order.

Automatic control of the unmanned aircraft is carried out in four channels: in the pitch channel θ – by means of elevator deflections δ_H, in the yaw channel ψ – by means of rudder deflections δ_V, in the roll channel ϕ – by means of aileron deflection δ_L, and in the speed channel V_0 – by changing the engine thrust δ_T.

Control laws of the UAV take the following form:

— in the pitch channel

$$\begin{aligned} T_3^H\dot{\delta}_H + T_2^H\delta_H &= K_{x_1}^H(x_1 - x_{1p}) + K_{z_1}^H(z_1 - z_{1p}) + K_U^H(U - U_p) \\ &\quad + K_W^H(W - W_p) + K_Q^H(Q - Q_p) + K_\theta^H(\theta - \theta_p) + \delta_{H0} \end{aligned} \tag{4.1}$$

— in the yaw channel

$$\begin{aligned} T_1^V\dot{\delta}_v + T_2^V\delta_V &= K_{y_1}^V(y_1 - y_{1p}) + K_V^V(V - V_{1p}) + K_W^V(W - W_p) \\ &\quad + K_R^V(R - R_p) + K_\psi^V(\psi - \psi_p) + \delta_{V0} \end{aligned} \tag{4.2}$$

— in the roll channel

$$\begin{aligned} T_1^L\dot{\delta}_L + T_2^L\delta_L &= K_\phi^L(\phi - \phi_p) + K_P^L(P - P_p) + K_V^L(V - V_p) \\ &\quad + K_R^L(R - R_p) + K_\psi^L(\psi - \psi_p) + \delta_{L0} \end{aligned} \tag{4.3}$$

— in the velocity channel

$$\begin{aligned} T_1^T\dot{\delta_T} + T_2^T\delta_T &= K_{x_1}^T(x_1 - x_{1p}) + K_U^T(U - U_p) + K_W^T(W - W_p) \\ &\quad + K_\theta^T(\theta - \theta_p) + K_Q^T(Q - Q_p) + K_R^T(R - R_p) + K_\psi^T(\psi - \psi_p) + \delta_{T0} \end{aligned} \tag{4.4}$$

where: T_i^j are time constants, K_i^j – amplification coefficients.

The designated control laws are non-integrable and impose restrictions on the motion system, and therefore they were considered as kinematic equations of non-holonomic constraints (Bloch, 2003; Ładyżyńska-Kozdraś, 2011; Nejmark and Fufajew, 1971). In the paper, the aforementioned equations were linked with the dynamic equations of motion of the unmanned aircraft vehicle, derived using analytical equations of mechanics in the form of the Bolzmann-Hamel equations with multipliers.

This approach made it possible to remove differences resulting from the dynamics of motion of the controlled object occurring between geometric, kinematic and dynamic preset parameters and their pursuance during the flight of the tested object.

5. General equations of motion of the unmanned aircraft vehicle – Boltzmann-Hamel equations for mechanical systems with non-holonomic constraints

Description of dynamics of the unmanned aircraft, treated as a non-deformable mechanical system, was made in the reference system rigidly connected with the $Oxyz$ object. In addition, control laws (4.1)-(4.4) were treated as non-holonomic constraints superimposed on motion of the system. Therefore, in order to determine the equations of motion, the Boltzmann-Hamel equations of motion of non-holonomic systems in the generalized coordinates (Graffstein *et al.*, 1997; Gutowski, 1971; Ładyżyńska-Kozdraś, 2011; Maryniak, 2005) were used.

From the Boltzmann-Hamel equations, after calculating the value of Boltzmann multipliers and determination of kinetic energy in quasi-velocities, a system of ordinary second-order differential equations was obtained:

— the equation of longitudinal motion

$$\begin{aligned}
&\frac{d}{dt}\Big(\frac{\partial T^*}{\partial U}\Big) - \frac{\partial T^*}{\partial V}R + \frac{\partial T^*}{\partial W}Q - \frac{\partial T^*}{\partial x_1}\cos\psi\cos\theta - \frac{\partial T^*}{\partial y_1}\sin\psi\cos\theta \\
&\quad + \frac{\partial T^*}{\partial z_1}\sin\theta + \frac{\partial T^*}{\partial \delta_H}\Big(QK_W^H - K_{x_1}^H\cos\psi\cos\theta + K_{z_1}^H\sin\theta - \frac{T_2^H}{T_1^H}K_U^H\Big) \\
&\quad + \frac{\partial T^*}{\partial \delta_V}\Big(QK_W^V - RK_V^V + K_{y_1}^V\sin\psi\cos\theta\Big) - \frac{\partial T^*}{\partial \delta_L}RK_V^L \\
&\quad + \frac{\partial T^*}{\partial \delta_T}\Big(QK_W^T - K_{x_1}^T\cos\psi\cos\theta - \frac{T_2^T}{T_1^T}K_U^T\Big) = Q_X
\end{aligned} \tag{5.1}$$

— the equation of lateral motion

$$\begin{aligned}
&\frac{d}{dt}\Big(\frac{\partial T^*}{\partial V}\Big)-\frac{\partial T^*}{\partial x_1}(\sin\phi\cos\psi\sin\theta-\sin\psi\sin\phi)\\
&\quad-\frac{\partial T^*}{\partial y_1}(\sin\phi\sin\psi\sin\theta+\cos\psi\cos\phi)\\
&\quad-\frac{\partial T^*}{\partial z_1}\sin\phi\cos\theta-\frac{\partial T^*}{\partial U}R+\frac{\partial T^*}{\partial W}P+\frac{\partial T^*}{\partial \delta_L}\frac{T_2^L}{T_1^L}K_V^L\\
&\quad+\frac{\partial T^*}{\partial \delta_H}[PK_W^H-K_{x_1}^H(\sin\phi\cos\psi\sin\theta-\sin\psi\sin\phi)-K_{z_1}^H\sin\phi\cos\theta\\
&\quad+RK_U^H]+\frac{\partial T^*}{\partial \delta_V}\Big[-PK_W^V+\frac{T_2^V}{T_1^V}K_V^V-K_{y_1}^V(\sin\phi\sin\psi\sin\theta+\cos\psi\cos\phi)\Big]\\
&\quad+\frac{\partial T^*}{\partial \delta_T}[-PK_W^T-K_{x_1}^T(\sin\phi\cos\psi\sin\theta-\sin\psi\sin\phi)+RK_U^T]=Q_Y
\end{aligned}\tag{5.2}$$

— the equation of climbing motion

$$\begin{aligned}
&\frac{d}{dt}\Big(\frac{\partial T^*}{\partial W}\Big)-\frac{\partial T^*}{\partial x_1}(\cos\phi\cos\psi\sin\theta+\sin\psi\sin\phi)\\
&\quad-\frac{\partial T^*}{\partial y_1}(\cos\phi\sin\psi\sin\theta-\cos\psi\sin\phi)\\
&\quad-\frac{\partial T^*}{\partial z_1}\cos\phi\cos\theta+\frac{\partial T^*}{\partial V}P-\frac{\partial T^*}{\partial U}Q+\frac{\partial T^*}{\partial \delta_L}PK_V^L\\
&\quad-\frac{\partial T^*}{\partial \delta_H}[(\cos\phi\cos\psi\sin\theta+\sin\psi\sin\phi)K_{x_1}^H\\
&\quad+(\cos\phi\cos\theta)K_{z_1}^H-\frac{T_2^H}{T_1^H}K_W^H+QK_U^H]\\
&\quad+\frac{\partial T^*}{\partial \delta_V}\Big[-PK_W^V+\frac{T_2^V}{T_1^V}K_V^V-(\cos\phi\sin\psi\sin\theta-\cos\psi\sin\phi)K_{y_1}^V\Big]\\
&\quad+\Big(\frac{T_2^V}{T_1^V}K_W^T+QK_U^T\Big)\frac{\partial T^*}{\partial \delta_T}=Q_Z
\end{aligned}\tag{5.3}$$

— the equation of roll motion

$$\begin{aligned}
&\frac{d}{dt}\Big(\frac{\partial T^*}{\partial P}\Big)-\frac{\partial T^*}{\partial \phi}+\frac{\partial T^*}{\partial U}(-RK_Q^H+VK_W^H)+\frac{\partial T^*}{\partial W}V-\frac{\partial T^*}{\partial V}W\\
&\quad+\frac{\partial T^*}{\partial R}Q-\frac{\partial T^*}{\partial Q}R+\frac{\partial T^*}{\partial \delta_V}(VK_W^V-WK_V^V+QK_R^V)\\
&\quad+\frac{\partial T^*}{\partial \delta_L}\Big(QK_R^L-K_\phi^L-WK_V^L+\frac{T_2^L}{T_1^L}K_P^L\Big)+\frac{\partial T^*}{\partial \delta_T}(VK_W^T-RK_Q^T)=Q_L
\end{aligned}\tag{5.4}$$

— the equation of pitch motion

$$
\begin{aligned}
&\frac{d}{dt}\Big(\frac{\partial T^*}{\partial Q}\Big)-\frac{\partial T^*}{\partial \phi}\sin\phi\tan\theta-\frac{\partial T^*}{\partial \theta}\cos\phi-\frac{\partial T^*}{\partial \psi}\frac{\sin\phi}{\cos\theta}-\frac{\partial T^*}{\partial W}U+\frac{\partial T^*}{\partial U}W\\
&\quad-\frac{\partial T^*}{\partial R}P+\frac{\partial T^*}{\partial P}R+\Big(WK_U^H+UK_W^H+K_\theta^H\cos\phi+\frac{T_2^H}{T_1^H}K_Q^H\Big)\frac{\partial T^*}{\partial \delta_H}\\
&\quad+\Big(-UK_W^V-PK_R^V+K_\psi^V\frac{\sin\phi}{\cos\theta}\Big)\frac{\partial^*}{\partial \delta_V}+(-RK_P^L+K_\phi^L\sin\phi\tan\theta)\frac{\partial T^*}{\partial \delta_L}\\
&\quad+\Big(-UK_W^T+WK_U^T+K_\theta^T\cos\phi-K_\psi^T\frac{\sin\phi}{\cos\theta}+\frac{T_2^T}{T_1^T}K_Q^T\Big)\frac{\partial T^*}{\partial \delta_T}=Q_M
\end{aligned}
\tag{5.5}
$$

— the equation of yaw motion

$$
\begin{aligned}
&\frac{d}{dt}\Big(\frac{\partial T^*}{\partial R}\Big)-\frac{\partial T^*}{\partial \phi}\cos\phi\tan\theta-\frac{\partial T^*}{\partial \theta}\sin\phi+\frac{\partial T^*}{\partial \psi}\frac{\sin\phi}{\cos\theta}+\frac{\partial T^*}{\partial V}U\\
&\quad-\frac{\partial T^*}{\partial U}V-\frac{\partial T^*}{\partial P}Q+\frac{\partial T^*}{\partial Q}P+\frac{\partial T^*}{\partial \delta_H}(-VK_U^H+K_\theta^H\sin\phi)\\
&\quad+\frac{\partial T^*}{\partial \delta_V}\Big(UK_V^V+\frac{T_2^V}{T_1^V}K_R^V-K_\psi^V\frac{\sin\phi}{\cos\theta}\Big)\\
&\quad+\frac{\partial T^*}{\partial \delta_L}\Big(QK_P^L+\frac{T_2^V}{T_1^V}K_R^L-K_\phi^L\cos\phi\tan\theta-K_\psi^L\frac{\sin\phi}{\cos\theta}\Big)\\
&\quad+\frac{\partial T^*}{\partial \delta_T}\Big(PK_Q^T+K_\theta^T\sin\phi-K_R^T\cos\phi\tan\theta-K_\psi^T\frac{\sin\phi}{\cos\theta}\Big)=Q_N
\end{aligned}
\tag{5.6}
$$

— the equation of elevator deflections

$$
\frac{d}{dt}\Big(\frac{\partial T^*}{\partial \dot{\delta}_H}\Big)-\frac{\partial T^*}{\partial \delta_H}=Q_{\delta H}
\tag{5.7}
$$

— the equation of direction rudder

$$
\frac{d}{dt}\Big(\frac{\partial T^*}{\partial \dot{\delta}_V}\Big)-\frac{\partial T^*}{\partial \delta_V}=Q_{\delta V}
\tag{5.8}
$$

— the equation of aileron motion

$$
\frac{d}{dt}\Big(\frac{\partial T^*}{\partial \dot{\delta}_L}\Big)-\frac{\partial T^*}{\partial \delta_L}=Q_{\delta L}
\tag{5.9}
$$

— the equation of drive unit

$$
\frac{d}{dt}\Big(\frac{\partial T^*}{\partial \dot{\delta}_T}\Big)-\frac{\partial T^*}{\partial \delta_T}=Q_{\delta T}
\tag{5.10}
$$

This set of equations constitutes, after the determination of kinetic energy and components of forces and moments of generalized forces, the general mathematical model of motion of the unmanned aircraft vehicle.

Kinetic energy of the flying object moving in any spatial motion, in the reference system $Oxyz$ associated with it, has been expressed in linear and angular quasi-velocities. Since the UAV is treated as a non-deformable object with movable control systems, its total kinetic energy is the sum of the kinetic energy of the object without surfaces of rudders and kinetic energy of particular control units.

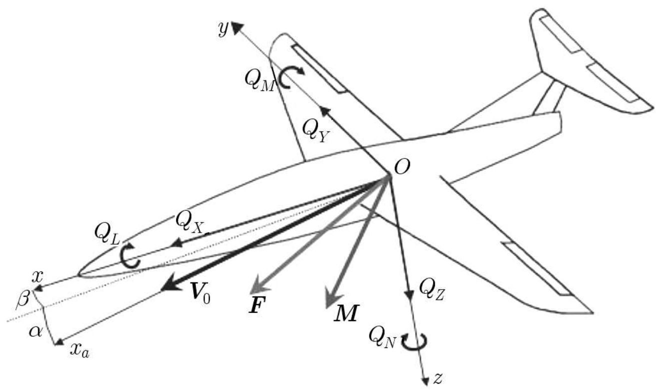

Fig. 3. Vectors of force and the moment of the external force as well as their components in the reference system $Oxyz$

Right sides of the equations create forces $\boldsymbol{F}$ and moments of forces $\mathfrak{M}$ generated by external loads acting on the object in the smooth configuration (Fig. 3), composed of forces and gravitational moments $\boldsymbol{Q}^g$, generated by the drive $\boldsymbol{Q}^T$, control $\boldsymbol{Q}^\delta$ and aerodynamic $\boldsymbol{Q}^a$ forces (Koruba and Ładyżyńska-Kozdraś, 2010; Ładyżyńska-Kozdraś, 2011; Nejmark and Fufajew, 1971). When determining the moments of forces acting on movable surfaces of rudders, the occurrence of moments from active forces generated by the drive of control elements (electric motor) ($\boldsymbol{M}_{HN}$, $\boldsymbol{M}_{VN}$, $\boldsymbol{M}_{LN}$), hinge moments ($\boldsymbol{M}_{HZ}$, $\boldsymbol{M}_{VZ}$, $\boldsymbol{M}_{LZ}$) and moments of forces generated by the inhibitory response resulting from the inertia of the system ($\boldsymbol{M}_{HR}$, $\boldsymbol{M}_{VR}$, $\boldsymbol{M}_{LR}$) are taken into account (Graffstein *et al.*, 1997; Ładyżyńska-Kozdraś, 2011).

The equations of motion of the unmanned aircraft, derived with the use of Boltzmann-Hamel equations (5.1)-(5.10) together with equations of nonholonomic constraints (4.1)-(4.4) and equations of kinematic correlations and guidance correlations (3.1)-(3.11), constitute the set of ordinary differential equations, with the use of which one may, at given initial conditions, determine

16 unknowns being a function of time determining the components of linear and angular velocity of the object U, V, W, P, Q, R, its temporary location on the route during the guidance x_1, y_1, z_1, ϕ, θ, ψ and angles of deflections of aerodynamic rudders δ_H, δ_V, δ_L, δ_T.

The preset flight parameters of UAV resulting from the adopted guidance method, (3.7)-(3.11), were included in equations of dynamics (5.1)-(5.10) through suitable amplification coefficients K_i^j in particular control channels. This way, they were included in the mathematical model of the UAV for conjugating parameters preset with the realized state of the flight. This revealed a close relationship of dynamic equations of motion of a controlled flying object with the laws of control and kinematic relations, which as a whole, form a system of nonholonomic constraints.

The equations derived in such a way make it possible to conduct mathematical calculations for controlled aircrafts: airplanes, unmanned aircrafts, rockets and aerial bombs (Koruba and Ładyżyńska-Kozdraś, 2010; Ładyżyńska-Kozdraś, 2008, 2011).

A separate issue is the proper selection of amplification coefficients in the control laws, which problem, still remaining in research (Blajer *et al.*, 2001; Graffstein, 2009), has been examined by the author, among others, in Ładyżyńska (2009). When selecting the reinforcement coefficients of the autopilot, an integral, quadratic criterion of quality control was used in the study, which complemented the assessment of transitional processes in all control channels

$$J = \sum_{i=1}^{4} \int\limits_{0}^{t_k} \Big[\frac{y_i(t) - y_{zi}(t)}{y_{i\,max}}\Big]^2 \, dt \tag{5.11}$$

where: $y_i(t)$ – stands for the actual course of the variable, $y_{zi}(t)$ – denotes the predetermined course of the variable, $y_{i\,max}$ is the maximum preset range of the i-th state variable or the preset value y_{zi} of the i-th state variable, if it takes a non-zero value.

6. Numerical simulation of guided UAV

Test numerical simulation of a guided UAV for newly designed *Waleń* unmanned aircraft, which is to be used as an airborne target, was carried out in the Technical Institute of Air Force (Fig. 4).

According to the diagram shown in Fig. 1, it has been assumed that a UAV moving along the preset trajectory in the first phase of simulation performs a

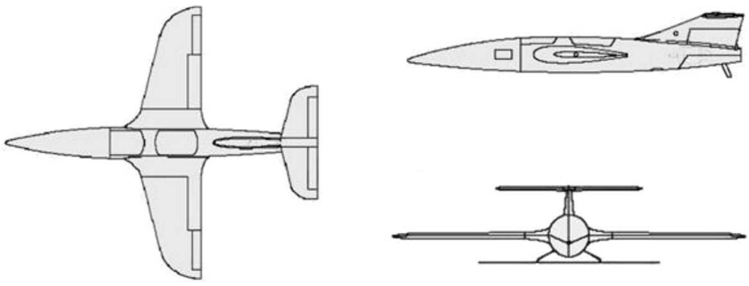

Fig. 4. Reference drawing of *Waleń* unmanned aircraft

steady flight rectilinear (at the speed $V_0 = 50\,\mathrm{m/s}$ at an altitude of 500 m), then bypasses the obstacle by climbing U-turn (no slip) with a change of altitude about 300 m, after which it returns to steady flight on the new altitude.

The coefficients of amplification appearing in control laws (4.1)-(4.4), took the following values:

$$
\begin{array}{lll}
K_{x_1}^H = -0.0029 & K_{z_1}^H = -0.008 & K_U^H = 0.0201 \\
K_W^H = -1.036 & K_Q^H = -2.3 & K_\theta^H = 0.3 \\
K_{y_1}^V = 0.0007 & K_V^V = -0.00054 & K_W^V = 0.0231 \\
K_R^V = 1.1 & K_\psi^V = -0.074 & \\
K_\phi^L = -0.0009 & K_P^L = 0.0007 & K_V^L = 0.0011 \\
K_R^L = -1.5 & K_\psi^L = -3.3 & \\
K_{x_1}^T = 1.06 & K_U^T = -3.004 & K_W^T = 0.22 \\
K_\theta^T = 4.1 & K_Q^T = -0.06 & K_R^T = 0.07 \\
K_\psi^T = -0.003 & &
\end{array}
$$

The results of simulation have been presented in a graphical way in Figs. 5--Figs. 8.

The correctness of performing the manoeuvre has been ensured through the coordinated use of deflections and by making a slip angle β impossible to occur. The analysis of graphs shows that the automatic control system ensures the maintenance of the desired flight trajectory, bringing the UAV on the right course ψ. For this purpose, it has proved necessary to increase the speed of flight depending on the angle of roll ϕ and to increase the angle of attack α. After performing the U-turn, the UAV maintains the values of flight parameters by returning to steady flight on the new course with the set new height.

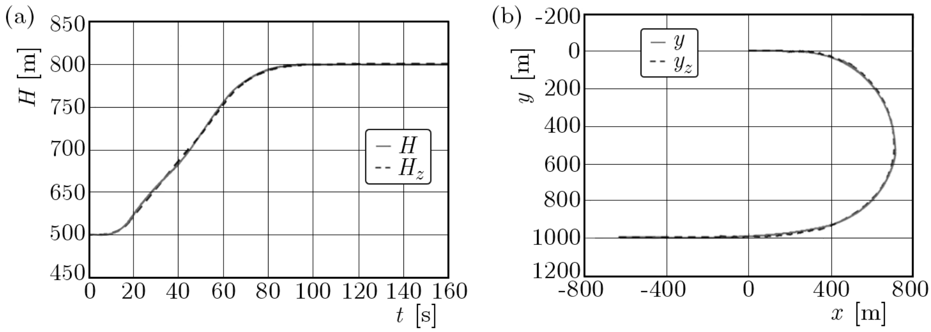

Fig. 5. Diagrams of the real and preset UAV flight altitudes (a) and lateral projections (b)

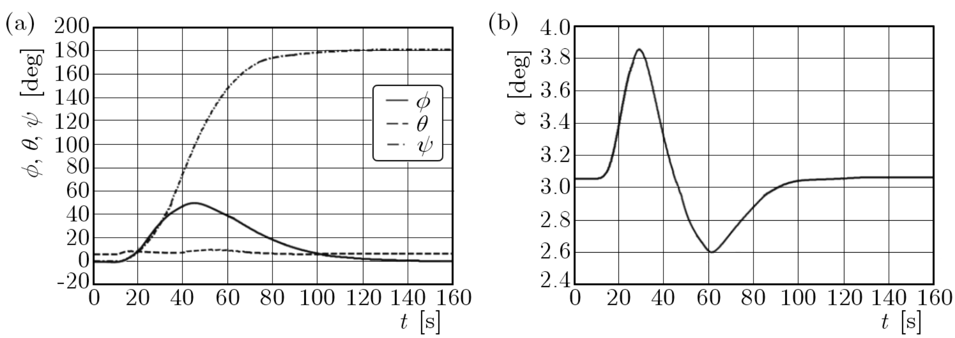

Fig. 6. History of the angles of roll, pitch, yaw (a) and the angle of attack (b)

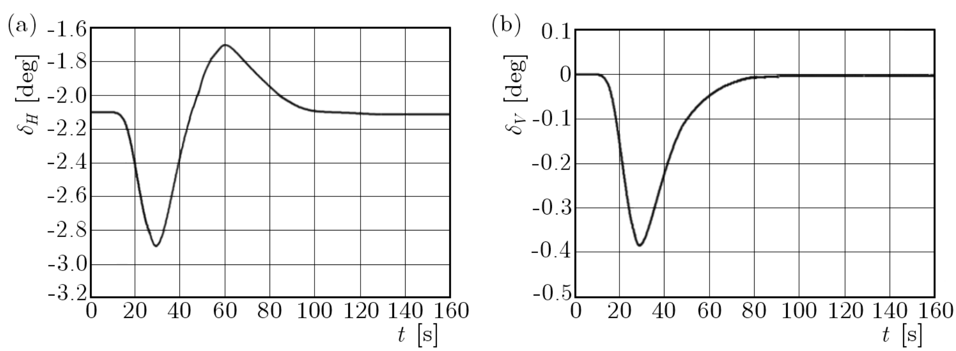

Fig. 7. History of the elevator (a) and rudder (b) deflection

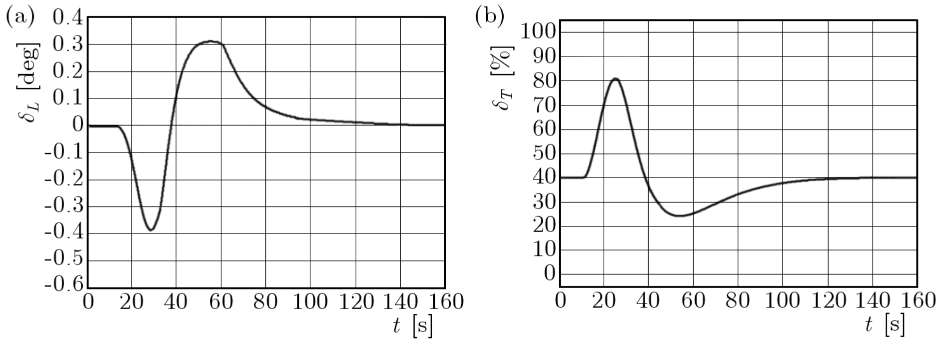

Fig. 8. History of the aileron deflection (a) and the changing engine thrust (b)

7. Conclusions

The use of the Boltzmann-Hamel equations for mechanical systems with nonholonomic constraints made it possible to develop the model of dynamics of the flight of unmanned aircraft. Using the control laws as kinematic correlations of deviations from the preset ideal guidance parameters, the control laws have been linked with dynamic equations of motion of unmanned aircraft vehicle.

The obtained simulation results show the correctness of the developed mathematical model. The flight of the unmanned aircraft takes place in a proper manner. It maintains the preset parameters resulting from the adopted guidance method throughout the entire flight.

The developed mathematical model and simulation program are universal and can be easily adapted to simulation, guidance and calculations of any unmanned aircraft vehicle (after proper parametric identification of the tested object).

A reliable UAV simulation process which can be adapted for different aircrafts would provide a platform for developing autopilot systems with reduced dependence on expensive field trials. In many cases, the testing of newly developed autopilot systems in a virtual environment is the only way to guarantee absolute safety. Additionally, the model would allow better repeatability in testing, with controlled flying environments.

References

1. Bloch A.M., 2003, *Nonholonomic Mechanics and Control. Systems and Control*, Springer, New York

2. Blajer W., 1998, *Metody dynamiki układów wieloczłonowych*, Monografie nr 35, Wydawnictwo Politechniki Radomskiej, Radom

3. Blajer W., Graffstein J., Krawczyk M., 2001, Prediction of the dynamic characteristics and control of aircraft in prescribed trajectory flight, *Journal of Theoretical and Applied Mechanics*, **39**, 1, 79-103

4. Chelaru T., Pana V., Chelaru A., 2009, Dynamics and flight control of the UAV formations, *Journal WSEAS Transactions on Systems and Control*, **4**, 4

5. Dogan A., Venkataramanan S., 2005, Nonlinear control for reconfiguration of unmanned-aerial-vehicle formation, *Journal of Guidance, Control, and Dynamics*, **28**, 4

6. Ducard G.J.J., 2009, *Fault-Tolerant Flight Control and Guidance Systems: Practical Methods for Small Unmanned Aerial Vehicles*, Advances in Industrial Control Series, Springer

7. Etkin B., Reid L., 1996, *Dynamics of Flight. Stability and Control*, John Wiley & Sons Inc., New York

8. Graffstein J., 2009, Wpływ parametrycznej niepewności modelu na zmiany współczynników wzmocnień automatycznej stabilizacji samolotu, *Prace Instytutu Lotnictwa*, **201**, 65-75

9. Graffstein J., Krawczyk M., Maryniak J., 1997, Ogólny model dynamiki automatycznie sterowanego samolotu bezpilotowego „ĆMA”, *Materiały IV Konferencji „Układy mechaniczne – teoria i zastosowania”*, Łódź, 211-216

10. Gutowski R., 1971, *Mechanika analityczna*, PWN, Warszawa

11. Jordan T.L., Foster J.V., et al., 2006, AirSTAR, *A UAV Platform for Flight Dynamics and Control System, NASA Langley Research Center*, Report Number: AIAA Paper 2006-3307: 8

12. Koruba Z., Ładyżyńska-Kozdraś E., 2010 The dynamic model of combat target homing system of the unmanned aerial vehicle, *Journal of Theoretical and Applied Mechanics*, **48**, 3, 551-566

13. Ładyżyńska-Kozdraś E., 2008, Analiza dynamiki przestrzennego ruchu rakiety sterowanej automatycznie, [In:] *Mechanika w Lotnictwie ML-XIII 2008*, J. Maryniak (Edit.), PTMTS, Warszawa

14. Ładyżyńska-Kozdraś E., 2009, The control laws having a form of kinematic relations between deviations in the automatic control of a flying object, *Journal of Theoretical and Applied Mechanics*, **47**, 2, 363-381

15. Ładyżyńska-Kozdraś E., 2011, *Modelowanie i symulacja numeryczna ruchomych obiektów mechanicznych skrępowanych więzami nieholonomicznymi w postaci praw sterowania*, Prace naukowe: Mechanika, z. 237, Oficyna Wydawnicza Politechniki Warszawskiej, Warszawa

16. Maryniak J., 2005, Dynamika lotu, [In:] *Mechanika techniczna, Tom II – Dynamika układów mechanicznych*, J. Nizioł (Edit.), Komitet Mechaniki PAN, IPPT PAN, Warszawa, 363-472

17. Nejmark J.I., Fufajew N.A., 1971, *Dynamika układów nieholonomicznych*, Państwowe Wydawnictwo Naukowe, Warszawa

18. Ou Q., Chen X.C., Park D., Marburg A., Pinchin J., 2008, Integrated flight dynamics modelling for unmanned aerial vehicles, *Proceedings of the Fourth IEEE/ASME International Conference on Mechatronic and Embedded Systems and Applications (MESA08)*, ISBN: 978-1-4244-2368-2, Beijing, China, 570-575

19. Rachman E., Razali R., 2011, A mathematical modeling for design and development of control laws for unmanned aerial vehicle (UAV), *International Journal of Applied Science and Technology*, **1**, 4

20. Sadraey M., Colgren R., 2005, UAV flight simulation: credibility of linear decoupled vs. nonlinear coupled equations of motion, *AIAA Modeling and Simulation Technologies Conference and Exhibit*, San Francisco, California

21. Shim D.H., Kim H.J., Sastry S., 2003, A flight control system for aerial robots: algorithms and experiments, *IFAC Control Engineering Practice*

22. Ye Z., Bhattacharya P., Mohamadia H., Majlesein H., Ye Y., 2006, Equational dynamic modeling and adaptive control of UAV, *Proceedings of the 2006 IEEE/SMC International Conference on System of Systems Engineering*, Los Angeles, CA, USA, 339-343

Modelowanie i symulacja numeryczna automatycznie sterowanego bezzałogowego statku powietrznego skrępowanego więzami nieholonomicznymi

Streszczenie

W pracy zaprezentowano modelowanie dynamiki lotu automatycznie sterowanego bezzałogowego statku powietrznego z zastosowaniem równań Boltzmanna-Hamela dla układów mechanicznych o więzach nieholonomicznych. Prawa sterowania potraktowano jako więzy nieholonomiczne nałożone na dynamiczne równania ruchu BSP. Uzyskano model matematyczny zawierający sprzężenie dynamiki statku powietrznego z nałożonym sterowaniem, wprowadzając związki kinematyczne jako parametry zadane ruchu wynikające z procesu naprowadzania. Poprawność opracowanego modelu matematycznego potwierdziła przeprowadzona symulacja numeryczna.

Manuscript received December 28, 2010; accepted for print June 14, 2011